

## Mixing of Liquids in Microfluidic Devices

Bruce A. Finlayson  
Professor Emeritus of Chemical Engineering  
University of Washington  
<http://courses.washington.edu/microflo/>

The mixing of liquids in eleven different microfluidic devices was characterized by a group of eleven students in chemical engineering during Spring quarter, 2008. The goal was to characterize in a uniform manner the flow and mixing that occurred in slow, laminar flow. Mixing of a dilute chemical in another liquid during slow, laminar flow is a particularly difficult task, but the results showed that for Reynolds number of 1.0 the amount of mixing depended mainly on the flow length divided by the Peclet number, for all geometries. Two-dimensional simulations frequently gave a good approximation of the three-dimensional simulations, and the optical variance (as measured by fluorescence) is not too different from the flow variance (sometimes called the mixing cup variance). The research group is shown in Figure 1. All simulations were done using Comsol Multiphysics.



**Figure 1. Research Group on Mixing, Dreyfus Scholars, Spring, 2008**

## 1. Flow and Convection Diffusion Equations

The equations are solved in non-dimensional form. The Navier-Stokes equation is

$$\mathbf{u} \cdot \nabla \mathbf{u} = -\nabla p' + \frac{1}{Re} \nabla^2 \mathbf{u}$$

Boundary conditions are no slip on the solid walls, specified velocity profile on the inlet boundary, and assigned pressure on the outlet boundary. Sometimes the inlet velocity profile was the fully developed one and sometime it was uniform; this made little difference.

The convective diffusion equation is valid for a dilute concentration in the carrier fluid; since the concentration is dilute, the viscosity of the total fluid does not change and the flow is unaffected by the concentration of the dilute material.

$$\mathbf{u} \cdot \nabla c = \frac{1}{Pe} \nabla^2 c$$

The boundary conditions are zero flux on solid walls, convective flux on the outlet boundary, and a concentration split on the inlet boundary: zero in one half and 1.0 in the other half. Thus, the average concentration at the inlet was 0.5. All simulations were done in Comsol Multiphysics, v. 3.4.

The average concentration at the exit was calculated using

$$c_{\text{mixing cup avg}} = \frac{\int_A c \cdot v dA}{\int_A v dA}$$

This should also be 0.5, by continuity, and differences from 0.5 were used to assess the accuracy of the calculations. The variance is then defined as

$$\sigma_{\text{mixing cup}}^2 = \frac{\int_A [c - c_{\text{mixing cup avg}}]^2 \cdot v dA}{\int_A v dA}$$

These are both referred to as mixing cup averages and mixing cup variances, since they account for the fact that the flow velocity in different regions of the outlet plane are different, and hence carry differing amounts of the dilute specie. In flow between flat plates, with concentration 1 on one half and zero in the other half, the variance is 0.25; this is then the maximum variance. In biological experiments, it is convenient to measure the average concentration by using fluorescence that measures the total amount of material in an optical path. It takes no account of

the differing velocities in different regions. Thus, optical averages and optical variances were also calculated.

$$c_{optical\ avg} = \frac{\int c dA}{\int_A dA} \quad \sigma_{optical}^2 = \frac{\int [c - c_{optical\ avg}]^2 dA}{\int_A dA}$$

The meaning of the variance is illustrated in Figure 2.

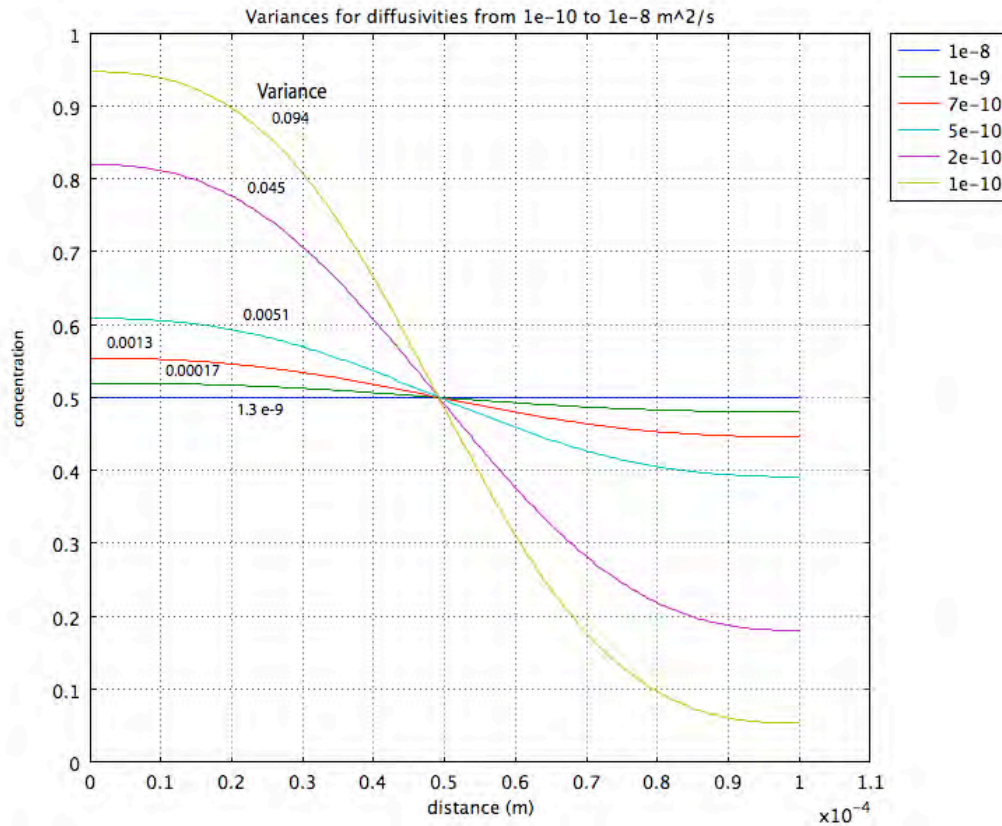


**Figure 2. Concentration profiles leading to different variances. Average concentration 0.5; velocity profile is parabolic.**

The focus was on slow flow, and the standard case was for a Reynolds number of 1.0 with variable Peclet numbers up to 1000 or 2000. The Reynolds number is defined as

$$Re = \frac{\rho u_s x_s}{\eta}$$

where  $\rho$  is the density and  $\eta$  is the viscosity. The velocity,  $u_s$ , is the average velocity entering the device. The distance,  $x_s$ , is a characteristic distance, usually the width of the entrance geometry; this must be identified for each geometry. For comparison purposes, we use water as the carrier fluid, so that  $\rho = 1000 \text{ kg/m}^3$  and  $\eta = 0.001 \text{ Pa s}$ . The base case velocity is taken as  $0.005 \text{ m s}^{-1}$

and the characteristic dimension was taken as 200  $\mu$ . This gives a Reynolds number of 1.0. The pressure drop is computed from the total pressure drop in the simulations,  $\Delta p'$ .

$$\Delta p(Pa) = \rho u_s^2 \Delta p'$$

The Peclet number is defined as

$$Pe = \frac{u_s x_s}{D}$$

where  $D$  is the diffusion coefficient or diffusivity. Note that  $Pe = Re Sc$ , where the Schmidt number is

$$Sc = \frac{\eta}{\rho D}$$

Peclet numbers from 10 to 1000 are used. When  $Pe = 1000$ , the diffusivity is

$$D = \frac{x_s u_s}{1000} = 10^{-9} \text{ m}^2$$

This is a reasonable value for typical organic chemicals, but biological molecules usually have smaller values, perhaps by a factor of 10-100. However, this was as low as we could go given the computer equipment available. Going to higher Peclet numbers requires a much finer mesh, which necessitates more memory than was available. However, as we see below, it is possible to predict the mixing for higher Peclet numbers based on calculations in shorter devices with lower Peclet numbers. This was tested, at least, within the range of  $10 \leq Pe \leq 1000$ .

## 2. Goals

The study is focused on situations with passive mixers (i.e. no mechanical mixing) at low Reynolds numbers. For a few of the geometries, inertial effects (at higher Reynolds numbers) are explored. Special geometries are necessary for this to be effective. Questions addressed for each geometry are:

- A. Do the variances collapse onto one curve if properly presented?
- B. Do your results follow the same curve of variance vs.  $z'/Pe$  as for a T-sensor?
- C. How different are the mixing cup and optical variances? Is this difference important?
- D. How do 2D and 3D results compare?
- E. What would you need to do in your device to reach a variance of 0.01? 0.001?
- F. What is the effect of Reynolds number? (This is pertinent only to a few of the geometries.)

### 3. Previous work

In work published previously<sup>1</sup>, the T-sensor (shown in Figure 3) is characterized as shown in Figure 4. Note that the variance roughly follows one curve, regardless of the Peclet number, provided the results are plotted versus  $z'/Pe$ . This is expected because the flow is basically straight down the device, except for the short entrance region, with diffusion sideways, and there is no convection sideways. Thus, diffusion controls the mixing, and the time in the device determines how far the material can diffuse. The parameter

$$\frac{z'}{Pe} = \frac{z}{x_s} \frac{D}{u_s x_s} = \frac{z/u_s}{x_s^2/D} = \frac{t_{flow}}{t_{diffusion}}$$

thus is a ratio of the characteristic time for flow in the axial direction to the time for diffusion in the transverse direction. Alternatively, one can examine the convective diffusion equation when there is no transverse velocity

$$w(x,y) \frac{\partial c}{\partial z} = D \left[ \frac{\partial^2 c}{\partial x^2} + \frac{\partial^2 c}{\partial y^2} + \frac{\partial^2 c}{\partial z^2} \right]$$

and deduce that axial diffusion term,  $D \partial^2 c / \partial z^2$ , can be neglected compared with the axial convection term,  $w \partial c / \partial z$ , since their ratio is proportional to  $1/Pe$ . To further validate this concept in 3D, Figure 5 shows a geometry with two pipes joining, and Figure 6 shows the variance as a function of  $z'/Pe$ ; data for the T-sensor and the two pipes joining essentially superimpose on each other.

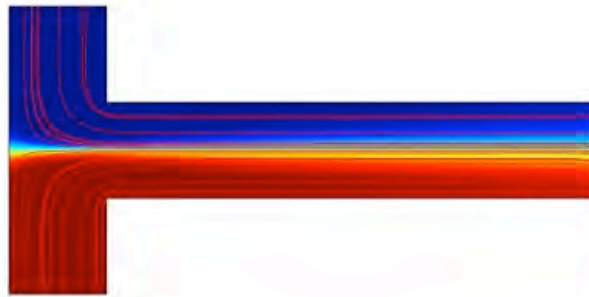


**Figure 3. T-sensor; lines are streamlines, color is concentration (red = 1, blue = 0)**

A similar result, dependence on mainly  $z'/Pe$ , was reported by Williams, *et al.*<sup>2</sup> for the herringbone mixer.

<sup>1</sup> Bruce A. Finlayson, Pawel W. Drapala, Matt Gebhardt, Michael D. Harrison, Bryan Johnson, Marlina Lukman, Suwimol Kunaridtipol, Trevor Plaisted, Zachary Tyree, Jeremy VanBuren, Albert Witarso, "Micro-component flow characterization," Ch. 8 in *Micro-Instrumentation*, (M. Koch, K. Vanden Bussche, R. Chrisman (ed.), Wiley, 2007).

<sup>2</sup> <http://www.rsc.org/Publishing/Journals/LC/article.asp?doi=b802562b>

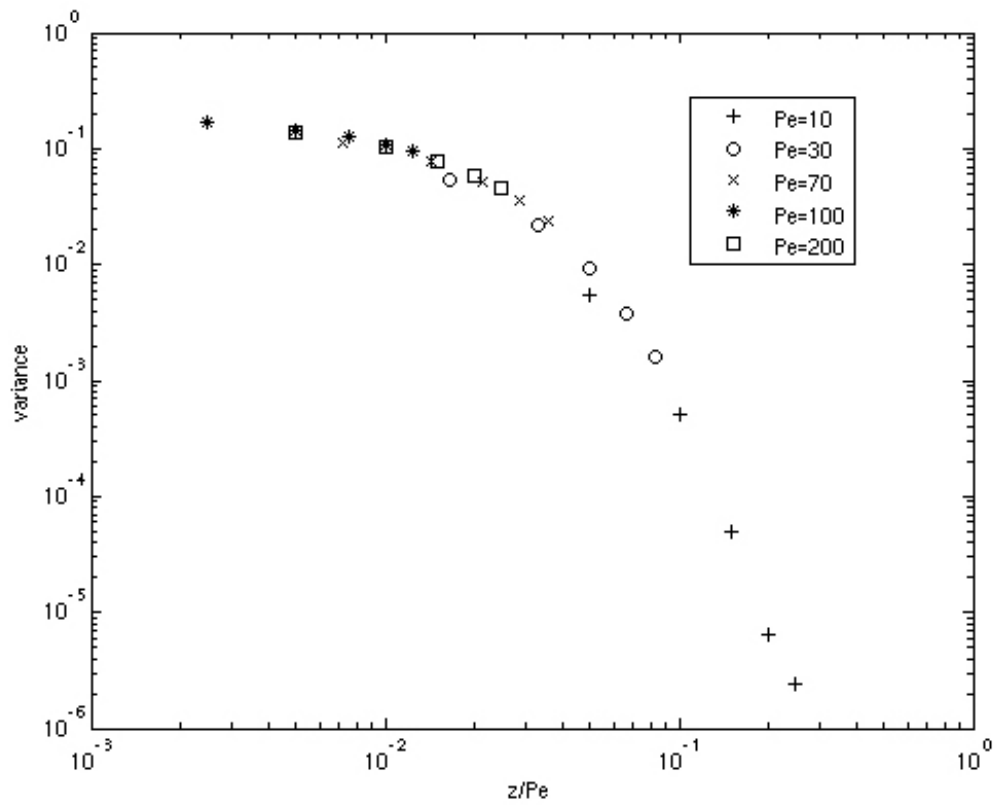


**Figure 4. Variance of T-sensor for Reynolds number = 1**

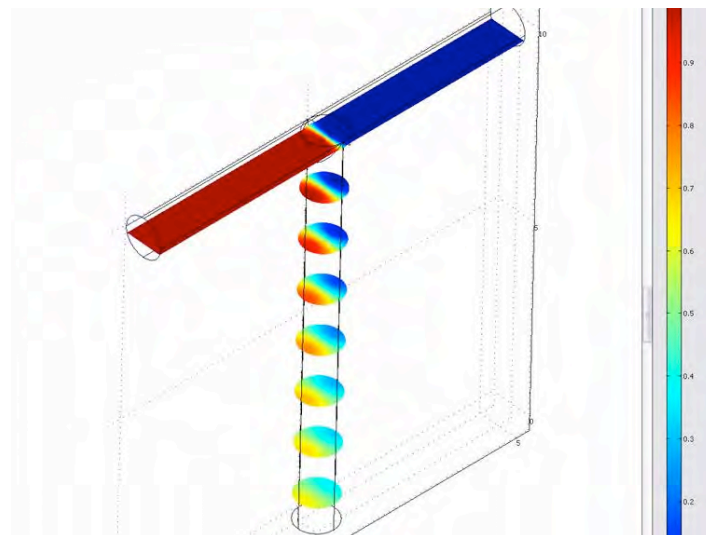


**Figure 5. Two pipes joining<sup>3</sup>**

<sup>3</sup> Daniel Kress, "Mixing Properties of a Microfluidic Device," Chem. Eng. 499 Project, Spring, 2007, [http://courses.washington.edu/microflo/index\\_Sp07.html](http://courses.washington.edu/microflo/index_Sp07.html).

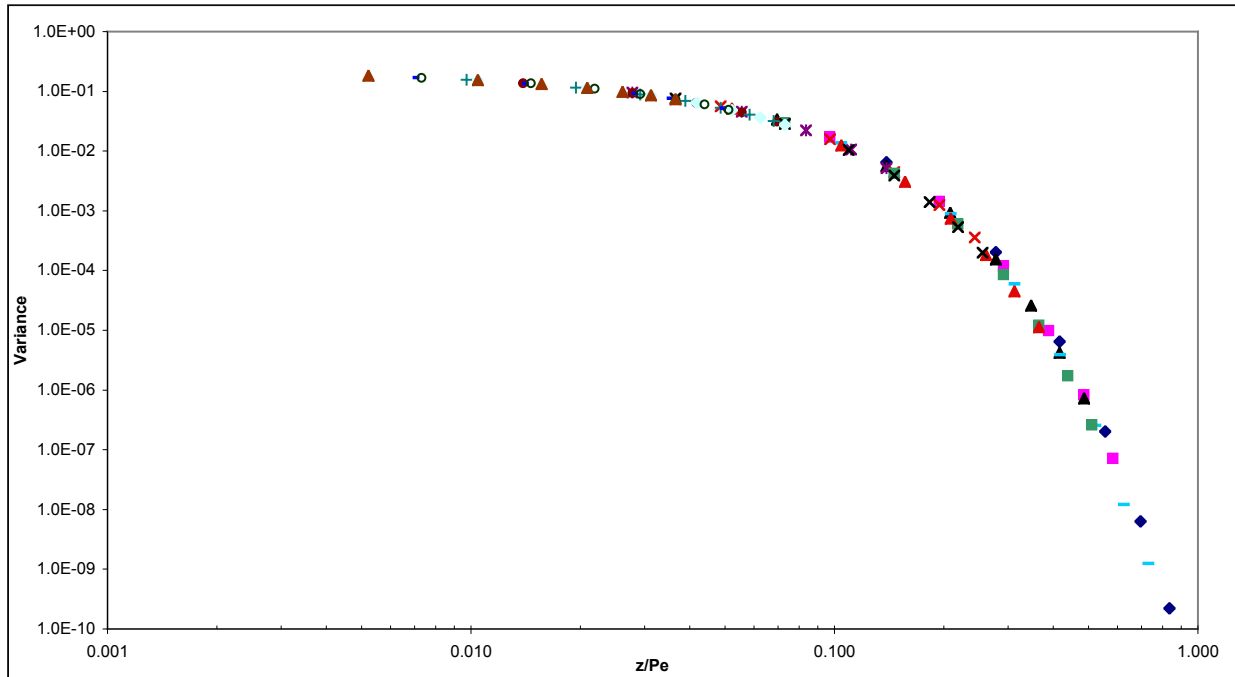


**Figure 6. Variance of mixing with two pipes joining and 2D T-sensor<sup>2</sup>**

Another example of mixing is for the serpentine mixer, discussed in Ref. 1 and Ref.<sup>4</sup> Figure 7 shows a typical concentration profile. In this case, enhanced mixing occurs due to the flow irregularities, even for a Reynolds number of 1.0. As shown elsewhere,<sup>1</sup> the serpentine mixer can be several hundred times shorter to achieve the same mixing as in a T-sensor. The progress of the mixing is shown step by step in Figure 8. Now the curves do not superimpose, but the general shape of them is similar.

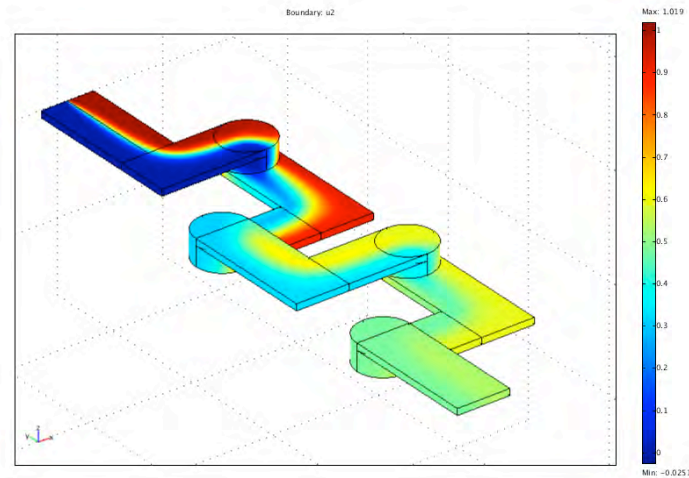


**Figure 7. Serpentine Mixer**

<sup>4</sup> Christopher Neils, Zachary Tyree, Bruce Finlayson, Albert Folch, “Combinatorial mixing of microfluidic streams”, Lab-on-a-Chip 4 342-350 (2004).

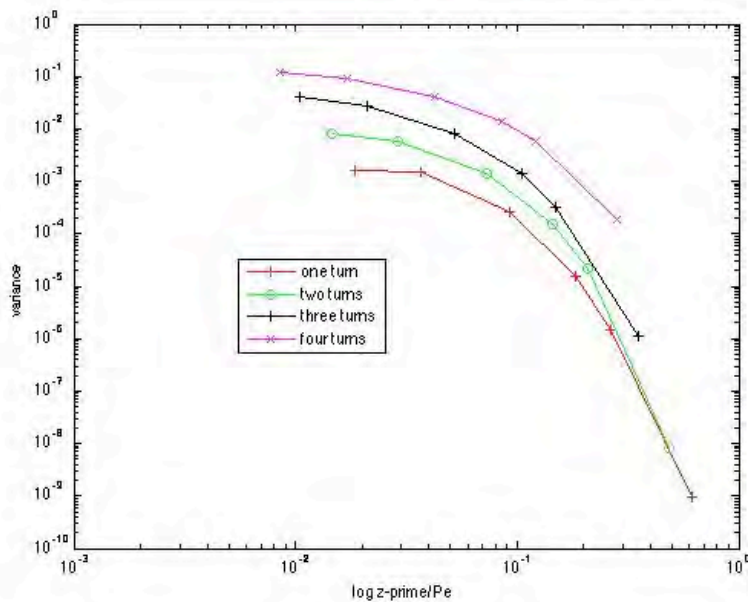
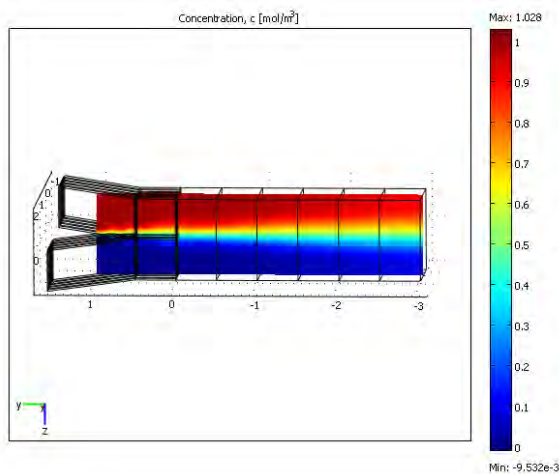


Figure 8. Variance in Serpentine Mixer,  $Re = 1$

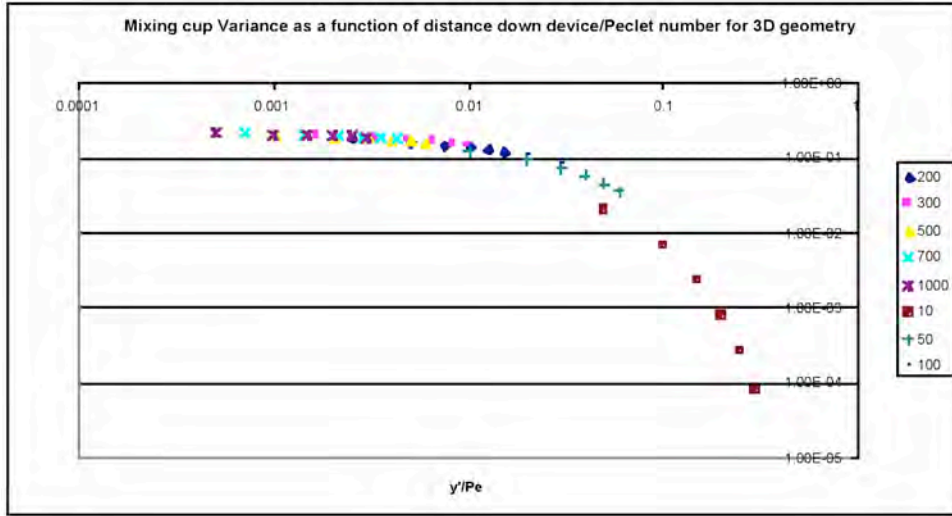
#### 4. Characterization of Diffusion in Microfluidic Devices

Eleven different geometries are characterized below. These geometries were taken from the literature. For each geometry, shown is a picture of the device, a picture of a solution, the plot of variance versus  $z'/Pe$ , and the pressure drop in Pa. The Reynolds number is 1.0 unless otherwise noted. The first set of geometries are for devices which are similar to the T-sensor; the other geometries introduce flow changes to create additional mixing. Full reports for each device are available (<http://courses.washington.edu/microflo/>).

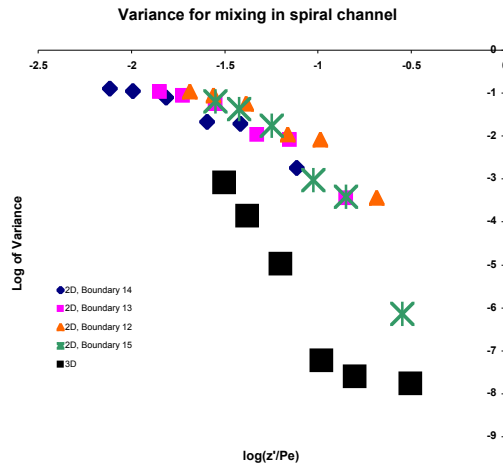
##### 4.1. "[Characterizing Mixing in a Lithographed Flow Device](#)"<sup>5</sup>, by Vann Brasher



<sup>5</sup> Hinsmann, *Lab Chip*, **1** 16 (2001)

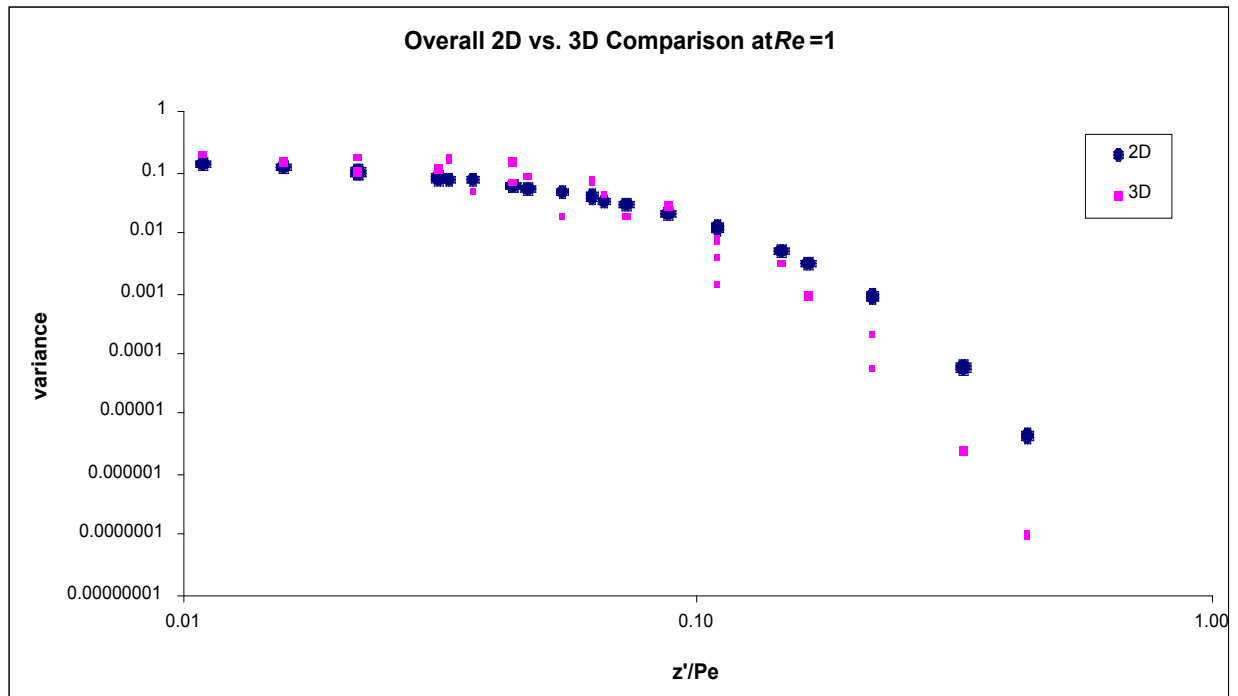
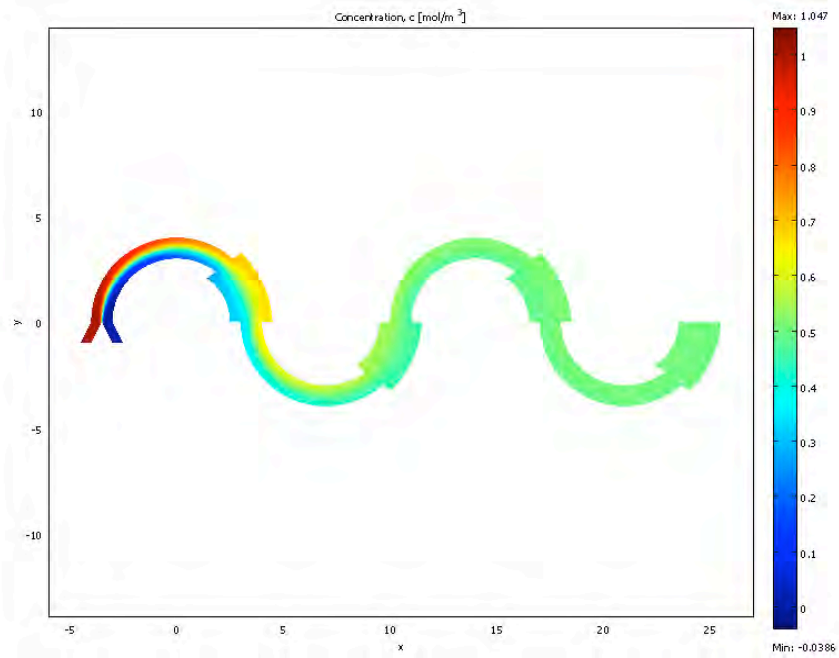


4.2. "[Mixing in Flow Devices: Spiral Channels](#)<sup>6</sup>," by Ha Dinh



<sup>6</sup> Sudarson, *Lab Chip*, 6 74 (2006)

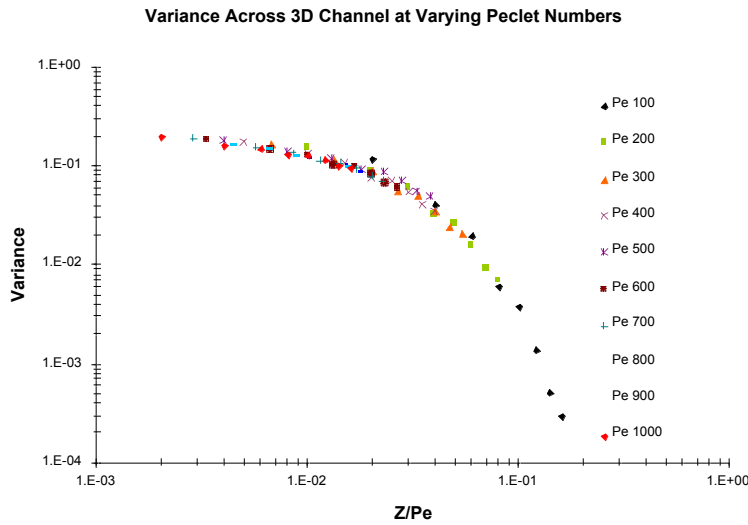
### 4.3. “[Micro-mixing by Rectangular Expansion Channel<sup>5</sup>](#),” by Ho Hack Song



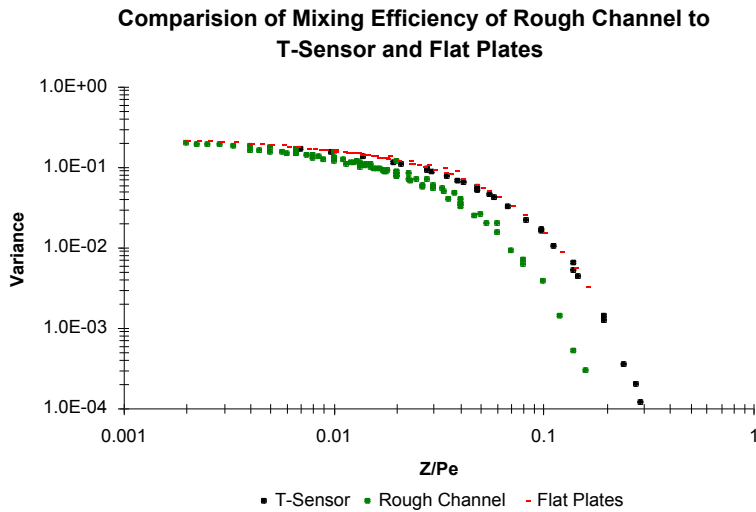
4.4. "[Mixing Efficiency in Rough Channels](#)<sup>7</sup>," by Francis Ninh



All geometries were assigned random ridges. The widths ( $W$ ) of the ridges were kept constant throughout each model but the height ( $H$ ) was determined randomly. All ridges extend down to a maximum of the width of the channel (1 unit). In (c) however, the ridges are allowed to extend above the bottom of the plate to a maximum of .6 units. (A)  $W$  of ridge = .5,  $H$  of ridge =  $n(.25)$  (B)  $W = .25$   $H = n(.25)$  (C)  $W = .25$ ,  $H = (n)*2$ , where  $n$  is a random integer and of values from 0 to a value where  $H$  was no greater than width of the inlet.

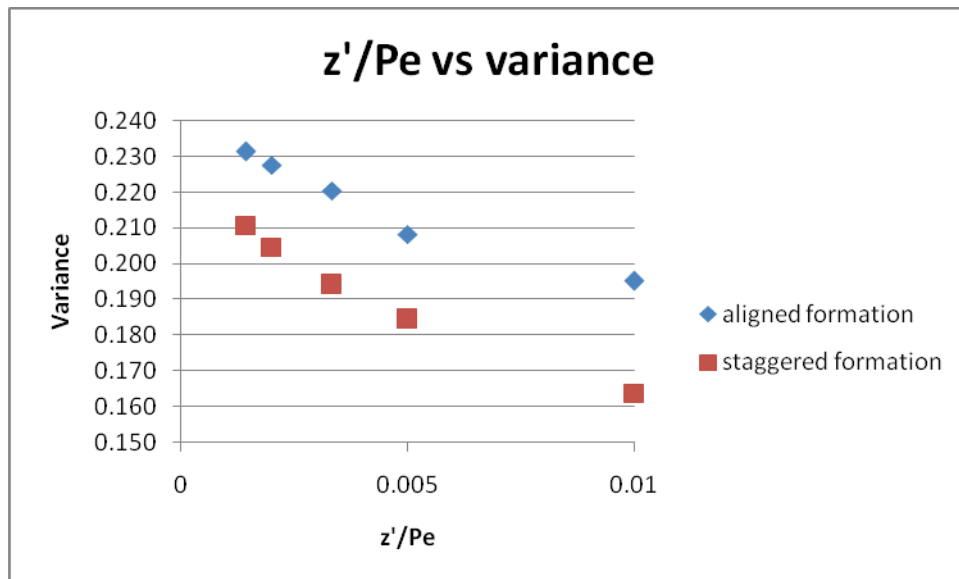
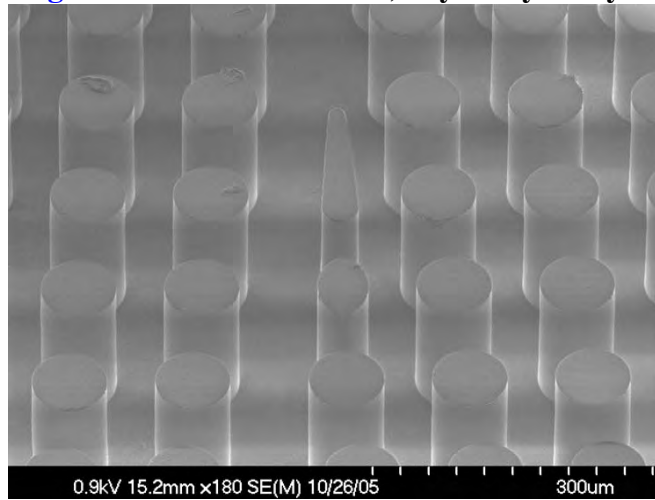


Variances all lie on one curve regardless of the Peclet number. That is, variances are essentially equivalent at the same  $z'/Pe$ .

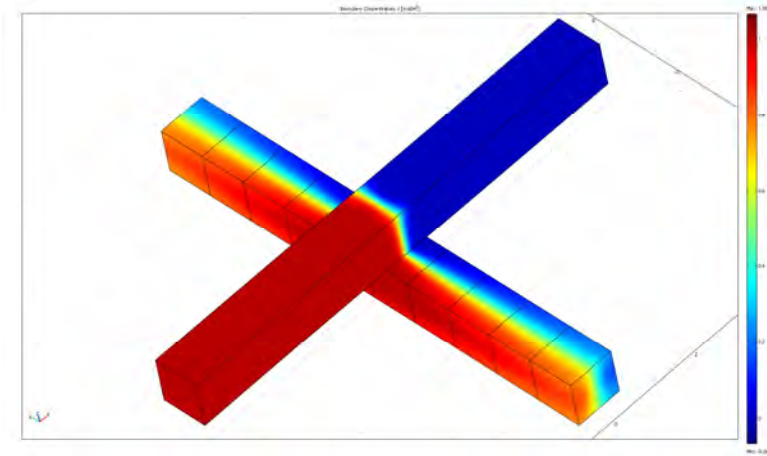


<sup>7</sup> Kiplik, *Phys. Fluids A*, **6** 1333 (1993)

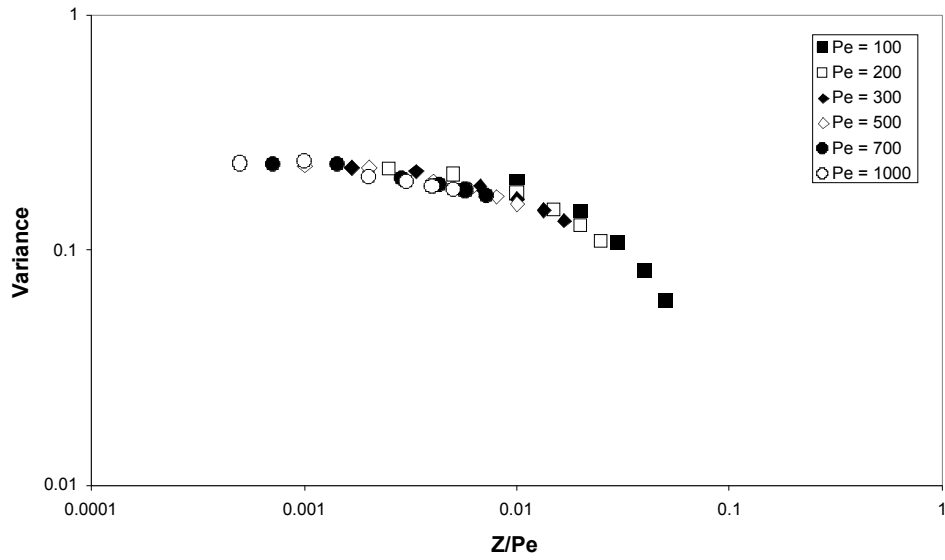
4.5. "[Micropillars Mixing in Microfluidic Devices](#)," by Andy Aditya



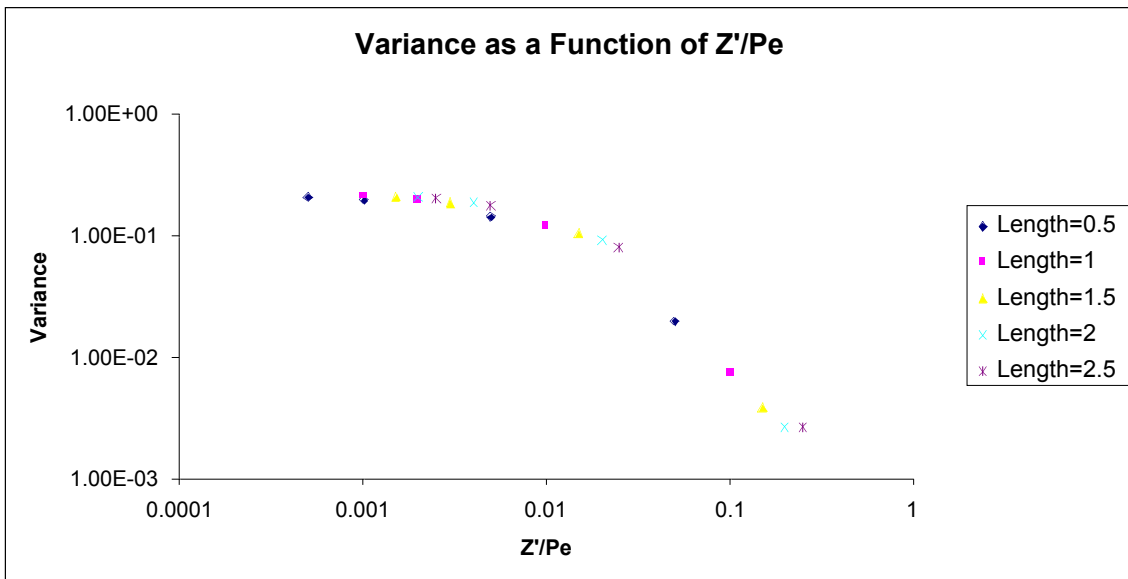
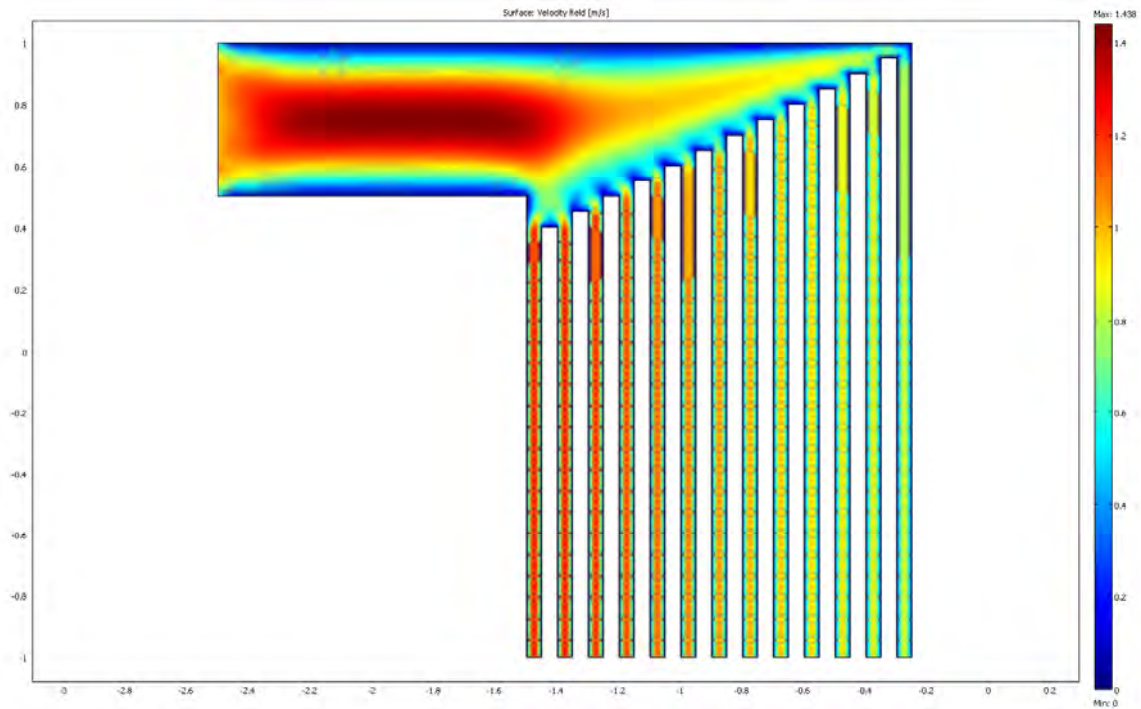
#### 4.6. "Flow in a Cross," by Adam Field



3-D Mixing in a Cross



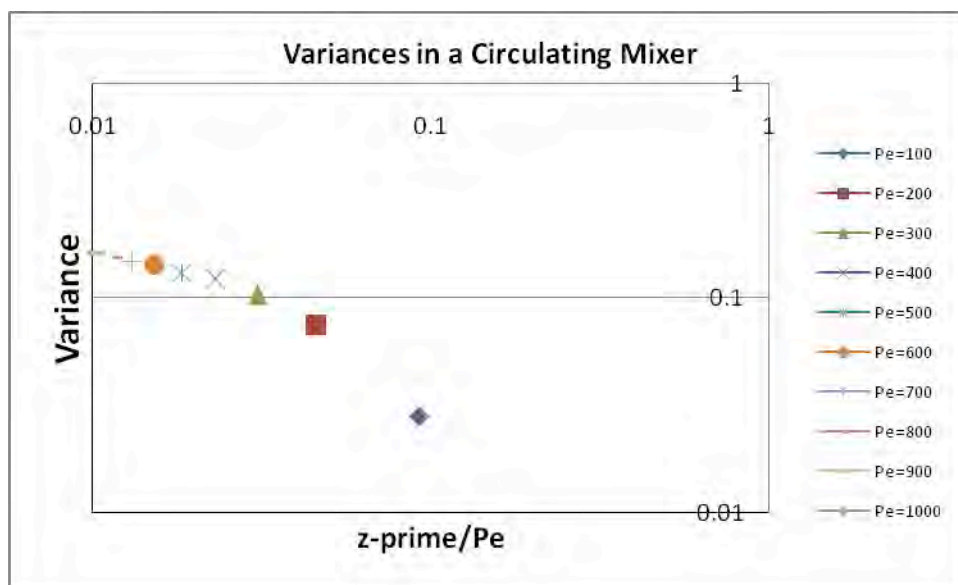
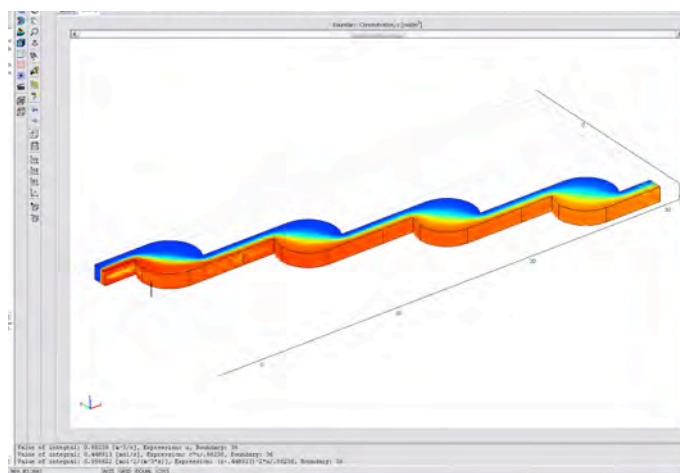
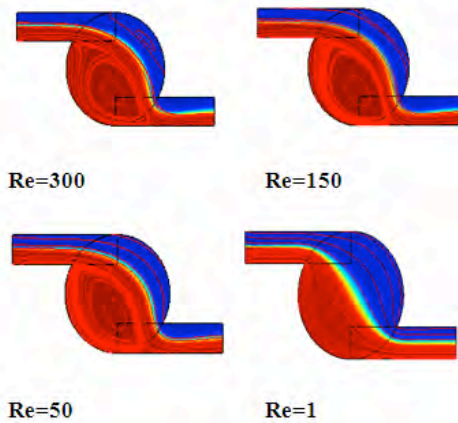
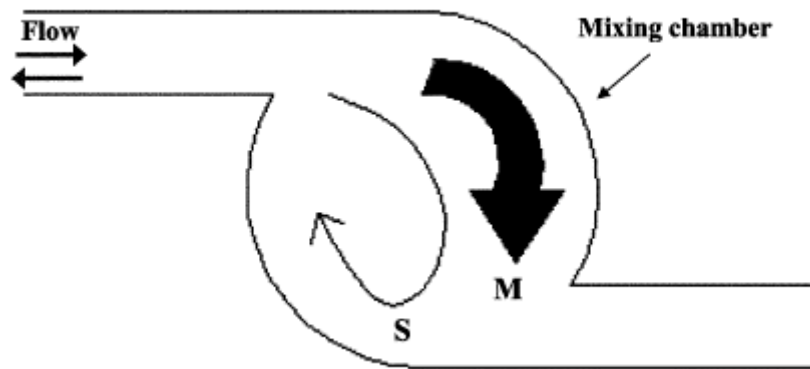
4.7. “Evaluation of Concentration Variance as a Function of  $z'/Pe^8$ ,” by Jordan Flynn



The Peclet numbers in this data were ranged from 10 to 1,000.

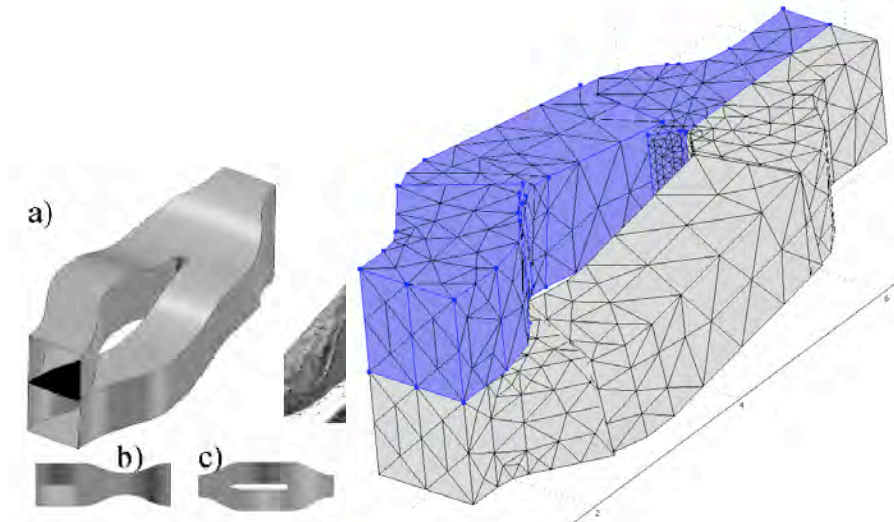
<sup>8</sup> Holden, *Sensors Actuators B*, **92** 199 (2003)

4.8. “Self Circulating Mixer Chamber<sup>9</sup>,” by Cindy Yuen

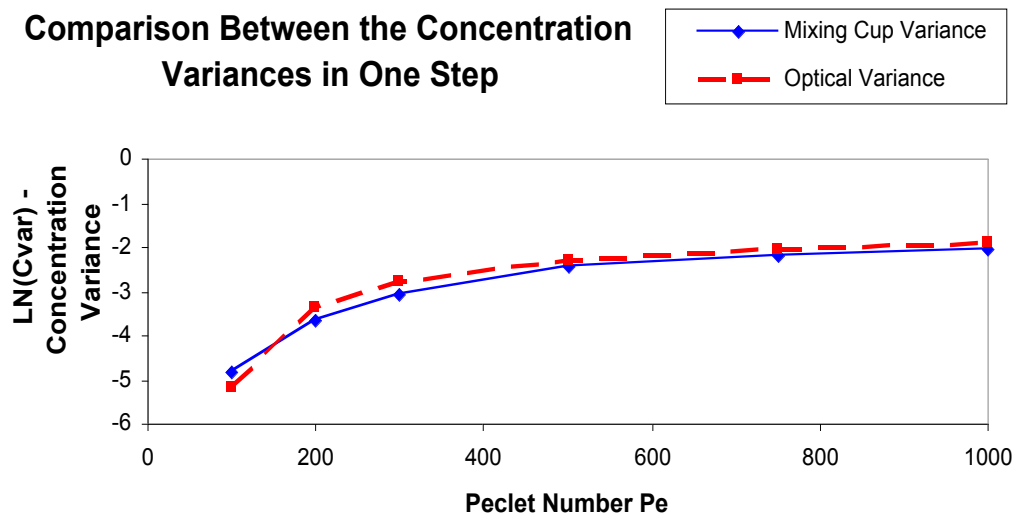


<sup>9</sup> Chung, *Lab Chip*, **4**, 70 (2004).

4.9. "[Mixing Properties of an Optimized SAR Mixer](#)<sup>10</sup>," by Lisa Dahl

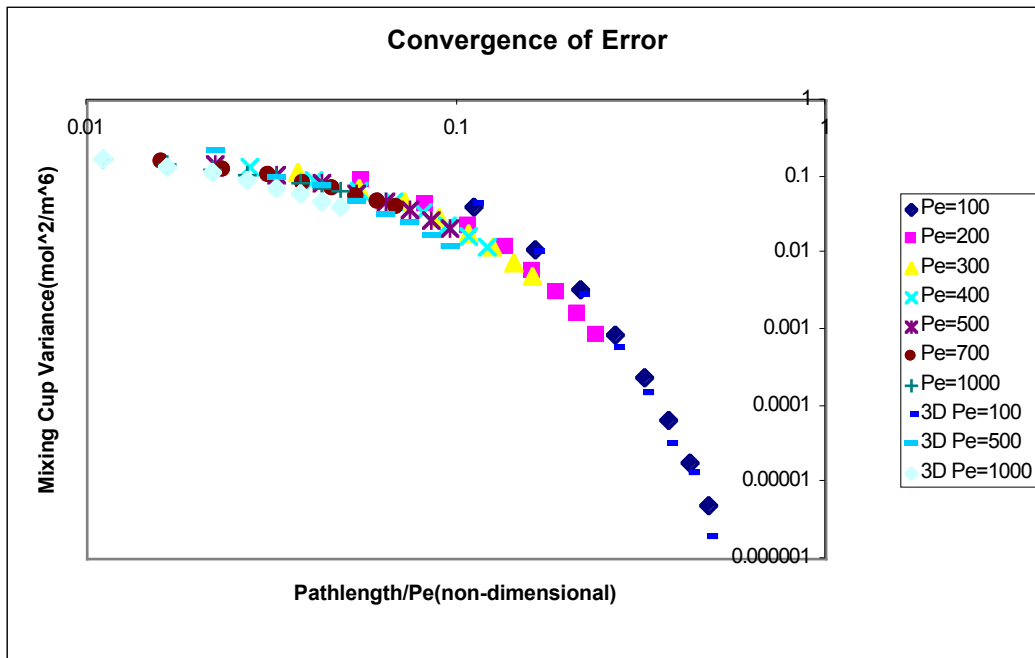
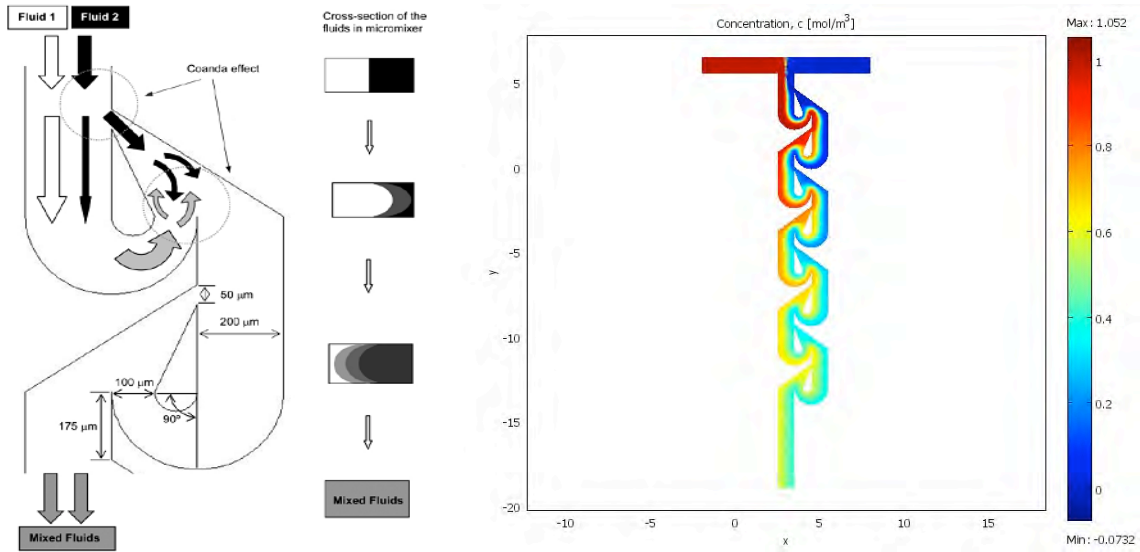


**Comparison Between the Concentration Variances in One Step**



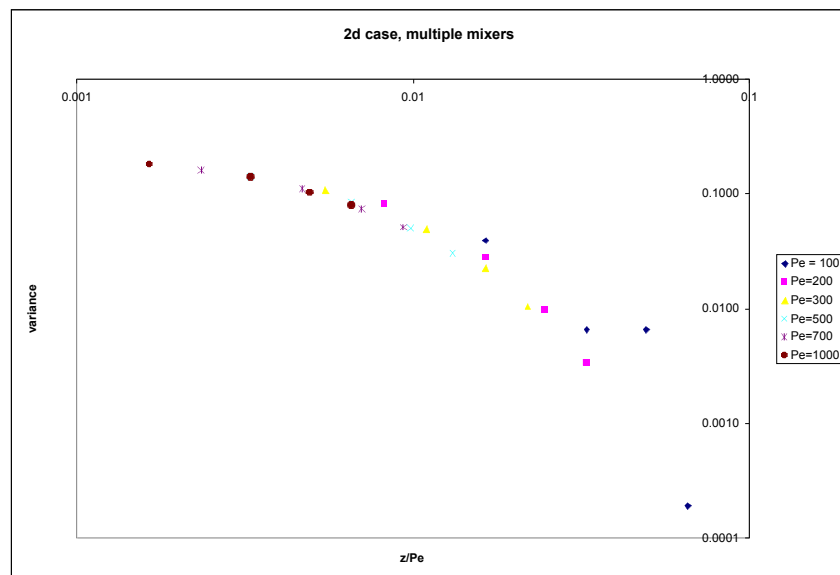
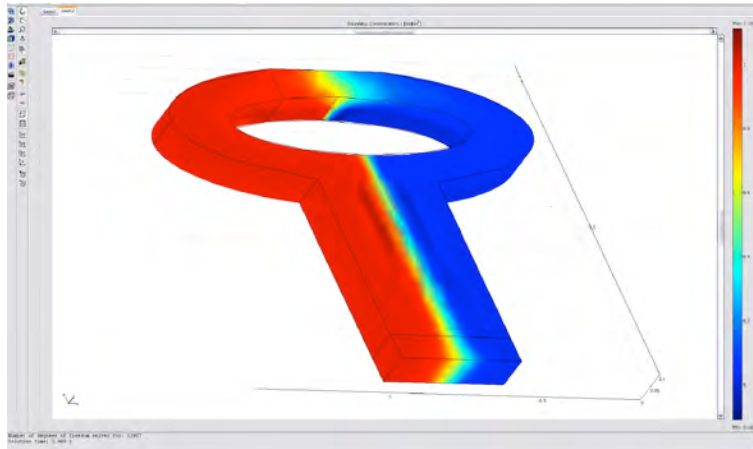
<sup>10</sup> Schonfeld, *Lab Chip*, 4 65 (2004)

4.10. "Microfluidic Research: Mixing Effectiveness of Modified Tesla Structures<sup>11</sup>," by Curtis Jensen



<sup>11</sup> Hong, *Lab Chip*, 4 109 (2004)

#### 4.11. "Folding Flow Mixers"<sup>12</sup>, by Andrew Nordmeier



## 5. Conclusion

The variance for each geometry, for  $Re = 1$ , fell on one curve as a function of  $z/Pe$ . The curve was similar in all cases, but shifted a bit for each device. The optical variances differed from the mixing cup variance somewhat, but not significantly on a logarithmic scale. Oftentimes the 2D simulations give a good representation of the 3D simulations; the cases when this doesn't hold is when the flow is particularly 3D in nature to induce mixing. If the device is similar to a T-sensor, increasing the Reynolds number makes little difference. The mixing is improved with increasing Reynolds number for geometries that induce laminar vortices based on inertial effects.

<sup>12</sup> micronit.com